

## Attraction of Minute Particles to Invariant Regions of Volume Preserving Flows by Transients

T. Shinbrot,\* M. M. Alvarez, J. M. Zalc, and F. J. Muzzio†

*Department of Chemical and Biochemical Engineering, Rutgers University, Piscataway, New Jersey 08854*  
(Received 13 June 2000)

We find that tracer material can be concentrated into invariant regions of flows due exclusively to transient effects, as are produced when tracers temporarily become more buoyant than the surrounding fluid. This can occur either as a single event, e.g., if the tracer is initially weakly buoyant, or under periodic forcing, e.g., when external effects (such as solar heating) change the tracer density periodically. We study both cases in experiments, in a model, and in direct numerical simulations of laminar flow in a stirred tank. Focusing occurs for very small tracer size and inertia in flows that are instantaneously strictly volume conserving.

DOI: 10.1103/PhysRevLett.86.1207

PACS numbers: 47.20.Ky, 05.45.-a, 47.54.+r

Localization and transport by fluids is of tangible, and sometimes pressing, importance. For example, recent experiments have shown that even modest material heterogeneities can produce dramatic changes in geothermal convection [1]. Similarly, the transport of greenhouse gases and other pollutants by oceanic [2] and atmospheric [3] currents is a subject of topical scrutiny, and recent measurements have revealed that gases can spontaneously concentrate into localized regions even under turbulent conditions [4]. Additionally, it is recognized that meandering oceanic eddies can persist over months and even years [5]. Thus there is evidence both that trace materials can be concentrated in volume preserving flows and that, once concentrated, they can remain trapped as they are transported across great distances. This is of importance in a broad range of fields, including biochemistry, where protein crystallization can be acutely sensitive to density fluctuations [6]; environmental engineering, where the separation of fine particles from gases is of increasing regulatory concern yet remains poorly understood [7]; and pharmaceuticals, where controlled delivery of aerosol drug preparations is a growing concern [8].

Because of its importance—and its fundamental curiosity—several groups of researchers have studied localization of particles in otherwise volume preserving flows [9,10]. To date, the mechanisms of localization have been confirmed in only one of two circumstances. First, large [7,8,11] or massive [9,12] particles are known to follow trajectories different from an ambient flow. These trajectories can be nonconservative, as has been observed in wake [7], channel [11], rotating, and other flows. Second, buoyant particles can rise until they reach a boundary of a flow, where they can be concentrated by subsurface currents [13].

In this Letter, we report on a new mechanism for focusing of material—either particulate or fluid—to invariant regions of an underlying volume preserving flow. In Fig. 1, we display results of a dye advection experiment in which colored dyes are injected into a tank of glycerine stirred by axisymmetric disks. Crucially, one dye in these experiments is not perfectly neutrally buoyant (de-

tails below), but was blended to be neutrally buoyant in a different batch of glycerine. We reproducibly find that the red, weakly buoyant, dye becomes concentrated onto structured chains of islands surrounding nested tori, while the

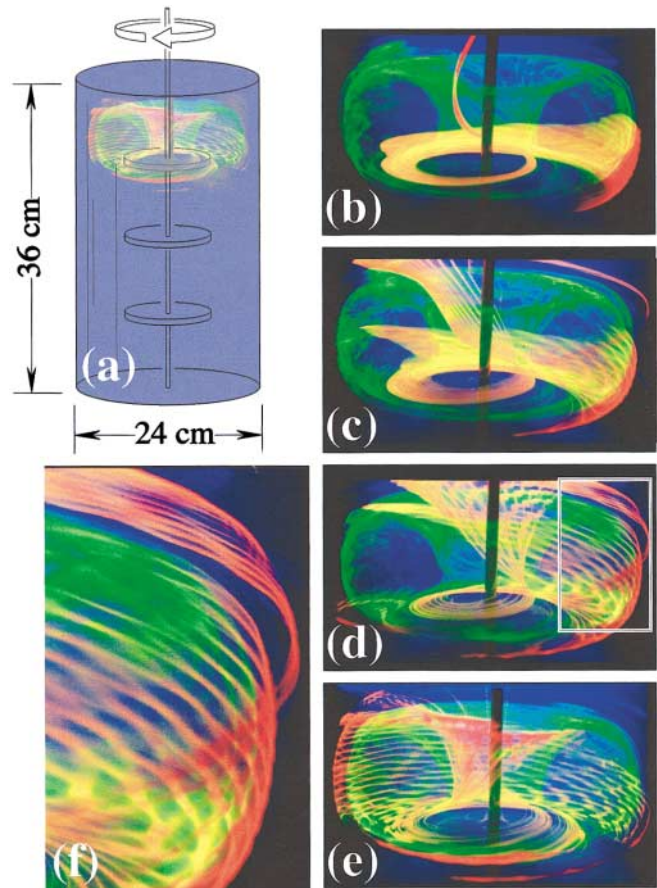


FIG. 1 (color). Transient focusing of dye onto island chains in a stirred tank of glycerine. (a) Tank stirred at Reynolds number ( $Re$ ) 20 by three axisymmetric disks. (b) Advection pattern of red dye 10 sec after injection near top of tank. Green dye was injected 2 min previously. (c), (d), (e) Red dye pattern 30, 60, and 90 sec after injection. (f) Enlarged view of red dye from (d). The tank is 36 cm high and 24 cm in diameter; the disks are 8 cm in diameter and 0.5 cm thick.

green, neutrally buoyant, dye injected earlier as nearly as possible into the same location in the same flow disperses uniformly onto a toroidal shell. Analysis (below) reveals that this is caused by transient effects and is not due to a steady buoyancy difference between dye and fluid. The existence of island chains is not remarkable; however, the reproducible attraction of the red dye alone to particular regions is unexpected.

This apparent attraction is quite rapid: In Figs. 1(b)–1(e) we show snapshots from a single experiment taken at successive times after injection of red dye [14]. Within 30 sec of injection, the dye fragments from a single ribbon [Fig. 1(b)] into multiple fine strands [1(c)], after which it relaxes onto two sets of island chains [1(e)]. Note that the dye has migrated to occupy two separate island chains *but is not found in the intervening fluid* (where nested toroidal shells reside), as shown also in an enlarged view [1(f)]. Subsequent experiments and numerical simulations (following) confirm that, almost independent of injection location or flow details, weakly buoyant dye invariably and rapidly finds its way to island chains.

The mechanism by which focusing by transients occurs can be described in its simplest context as follows. Consider the “traveling wave” map (1), which has been used to model atmospheric transport [15]:

$$\begin{aligned} y_{n+1} &= [y_n - 0.4 \sin(x_n)] \bmod 2\pi, \\ x_{n+1} &= [x_n + 0.4(y_{n+1}^2 - 1)] \bmod 2\pi. \end{aligned} \quad (1)$$

Although this model is very simple, the property of transient focusing is generic to any volume preserving system. The map (1) defines the transport of tracer locations  $(x_n, y_n)$  at discrete times,  $n$ , so if we distribute 500 points on a line within the domain  $(0, 2\pi) \times (0, 2\pi)$  and record positions of the points during 200 successive iterates of the map, we obtain the cumulative plot shown in Fig. 2(a). On the other hand, we can duplicate the effect of buoyancy on tracer particles by using the modified map:

$$\begin{aligned} y_{n+1} &= [y_n - 0.4 \sin(x_n) + C_n] \bmod 2\pi, \\ x_{n+1} &= [x_n + 0.4(y_{n+1}^2 - 1)] \bmod 2\pi, \\ C_{n+1} &= \Gamma C_n. \end{aligned} \quad (2)$$

Here the term  $C_n$  is intended to mimic the effect of net buoyant transport, and decays with rate  $\Gamma < 1$  due to dispersion of tracers [16]. Notice that at any instant in time,  $C_n$  is a constant, and for any constant  $C_n$  the mapping (2) is *strictly volume preserving*. Nevertheless, *because  $C_n$  changes with time*, the combined map (2) is *not* volume preserving. This can be verified by calculating the determinant of the Jacobian,  $|J|$ , of each map [17]: For constant  $C_n$ , the first two lines of map (2) identically give the conservative value  $|J| \equiv 1$ , yet the full map (2) gives a nonconservative  $|J| = \Gamma$ .

This model is sufficient to faithfully capture the focusing effect. This is shown in the time sequence Figs. 2(b)–2(d), where we track the most recent 200 iterates of the same

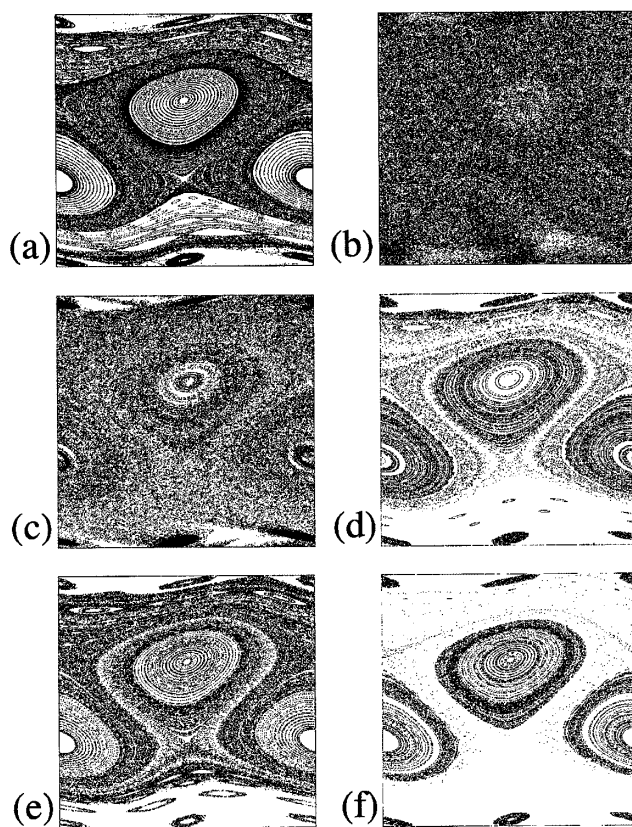


FIG. 2. (a) The 500 tracers tracked through 200 iterates of mapping (1), without an effective buoyancy term. (b)–(d) The same tracers tracked through iterates (b) 1–200; (c) 201–400; (d) 601–800 of mapping (2), with an effective buoyancy term. (e) One forcing cycle of mapping (2) at 1/100 of the initial amplitude used before; (f) 15 forcing cycles.

500 tracers as before, after successive iterates of map (2). The area covered by tracers at the resolution shown decreases by a factor of 2 between the base map [Fig. 2(a)] and the modified map after 800 iterates [18] [Fig. 2(d)].

In the context of this simple map, the mechanism by which focusing of tracers occurs can be understood in the following way. At any given time,  $n$ , the integrated distance that a tracer would move upward due to the buoyancy term alone is given by the geometric series

$$\sum_{i=n}^{\infty} C_i = C_n \sum_{j=0}^{\infty} \Gamma^j = \frac{C_n}{1 - \Gamma}. \quad (3)$$

Thus if a tracer lies in an island much farther than  $C_n / (1 - \Gamma)$  from its uppermost boundary, it cannot be removed from the island by buoyancy alone [19]. However, tracers outside of these islands can at any time enter them from below under the influence of the buoyant term. Moreover, since  $C_n$  diminishes over time, tracers typically become trapped in successively smaller islands as time progresses. This is borne out in Fig. 2: At 200 time steps, the tracer distribution is nearly uniform, but after 400 time steps, both the large central islands and the island chains at the top and bottom of the computational domain become densely populated at the expense of nearby, chaotic,

regions. By 800 time steps, smaller islands have become visible in a sea nearly depopulated of tracers.

We can confirm that this mechanism is at work in the physical problem displayed in Fig. 1 by performing direct numerical simulations with and without transient tracer buoyancy variations. In Fig. 3(a), we display locations of  $5 \times 10^5$  inertialess point tracer particles in a simulation [20] of the tank flow of Fig. 1(a). We initially place tracers on the surface of a small sphere approximately at the position of dye injection in the physical experiment. To simulate dye buoyancy, we add the velocity field obtained for the tank [21] to a vertical velocity given by  $V_{\text{buoy}} = -0.4e^{-t/8}$  cm/sec, where  $t$  is the elapsed time and the coefficients approximate experimental rise times of injected aliquots of red dye. In Fig. 3(b), we quantify the extent of tracer focusing by evaluating the difference between correlation functions from the simulations with and without transient tracer buoyancy. Correlations are diminished at length scales  $D_1$  and  $D_2$  [identified in Fig. 3(a)] of the base torus in favor of smaller length scales, confirming that transiently buoyant tracers do become focused from uniform locations around a torus to more localized positions.

Transient forcing can be strengthened by repeated application: In Figs. 2(e) and 2(f), we display tracers after 1 and 15 cycles in a simulation where once per unit time, tracer buoyancy is periodically reinitialized to the value  $C_0$  and allowed to decay at the rate  $\Gamma$ . At the resolution shown in Fig. 2 ( $486 \times 486$  pixels), the fractional area containing tracers reduces from 14% after 1 cycle of 800 iterates to 9% after 7 cycles. Because the decay toward islands is repeated, the buoyancy contrast between tracer and ambient velocities can be correspondingly diminished: In Figs. 2(e) and 2(f), for example,  $C_0$  is 1% of the value

[20] used in Figs. 2(b)–2(d). This may be relevant to geophysical flows where tracers are periodically heated, e.g., by solar or geothermal action.

Although we cannot perform experiments on geophysical scales, we can mimic periodic forcing in the laboratory, as follows. In Fig. 4 we display fine ( $50 \pm 10 \mu\text{m}$  diameter) spherical ferromagnetic particles suspended in a tall thin glass cylinder filled with glycerine. By using ferromagnetic particles, we can force the tracers without significantly altering the ambient flow. The system is stirred by a single shaft with a stepped diameter that generates a simple torus (intended to mimic long-lasting vortices seen in physical systems) above the step.

If a small permanent magnet is held fixed against the cylinder wall, nearly all of the particles can be captured, as seen near the magnet in Fig. 4(a). If no magnet is used, all of the particles settle to the container bottom. *In either steady configuration, no particles are found near the fluid torus.* However, *if the magnet is periodically placed against the cylinder and removed, the particles settle into asymptotic orbits surrounding invariant tori.* This is seen in Fig. 4(b), where we identify three particle-rich regions, one above the large upper torus, one below it, and a final region around a small torus, not otherwise evident, above a small setscrew, visible to the left of the shaft. None of these structures is visible under steady conditions. As a final example, in Fig. 4(c), we display the result of an experiment in which we periodically place the magnet near the bottom of the cylinder for an extended period, then slowly raise it to the top of the tank and remove it. The cloud of particles thereby released reveals structure within the tori as well as around them. Under this forcing protocol, tori are periodically revealed and then vanish as the particles

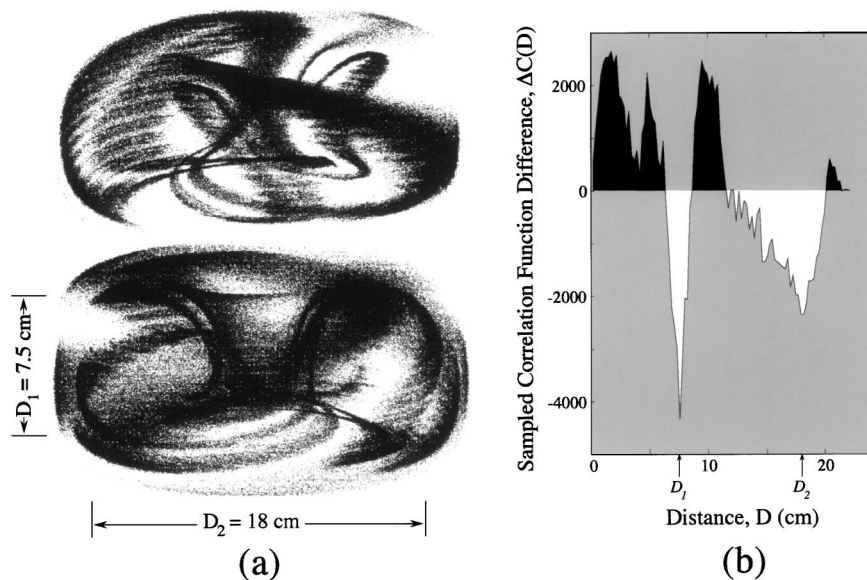


FIG. 3. (a) Direct numerical simulation of advection of  $5 \times 10^5$  tracers initially placed near the top of the tank studied in experiment [Fig. 1(a)]. Top figure displays advection after 160 impeller revolutions at  $\text{Re} = 20$  using tracers that experience decaying buoyancy as described in text; lower figure displays advection of ideal, nonbuoyant, tracers. (b) Difference between sampled [22] correlation functions for the two cases shown in (a).

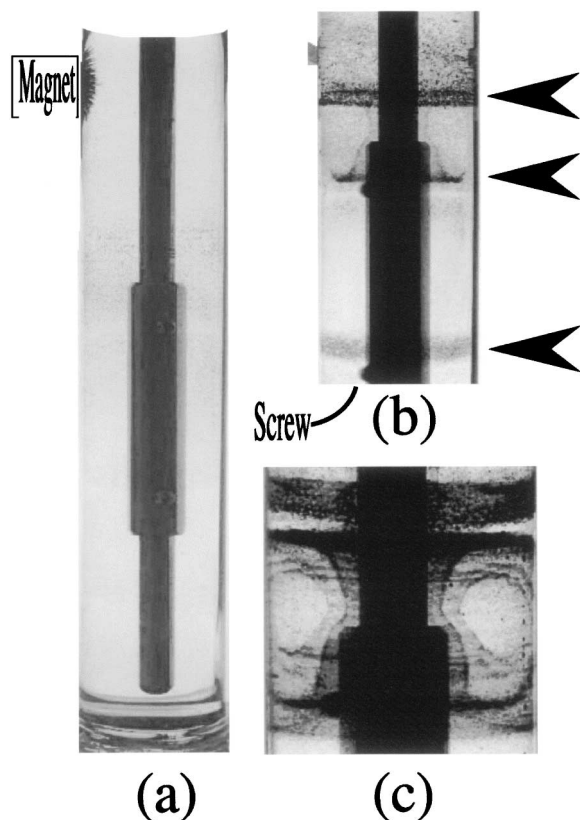


FIG. 4. Migration of fine ferromagnetic particles in glycerine under periodic and transient forcing. The tank is a 3.7 cm diameter, 29 cm high, glass tube, stirred at 300 rpm. (a) With magnet in fixed position, particles are cleared from fluid. (b) With magnet periodically placed and removed (the magnet is periodically placed against the tube for 1 min and removed for 2 min), particles migrate to the vicinity of toroidal regions of flow. (c) Expanded view of upper torus in experiment where magnet is used to periodically release clouds of particles from above.

condense onto the magnet, while under the previous protocol, the tori remain outlined by tracer particles throughout tens of forcing cycles (a comparable length of time).

In conclusion, we have identified a new effect that causes transiently forced tracers to become focused on invariant islands in volume preserving flows independent of tracer particle size or mass. The mechanism for this effect appears to be generic and causes tracers to become localized around invariant regions of fluid flows, *only* during transient (especially periodic) forcing. We anticipate that this may be of significance to many practical problems, such as those in geophysical flows that are either externally forced (e.g., oceanic or atmospheric systems) or that contain heterogeneities that become diluted over time.

We thank S. Cerbelli, J.D. Meiss, and Acusim Software, Inc., for valuable input, and Colgate-Palmolive Co., Fujitsu, Inc., and CONACyT for financial support.

\*Electronic address: shinbrot@sol.rutgers.edu

†Corresponding author.

Electronic address: muzzio@sol.rutgers.edu

- [1] For example, A. Davaille, *Nature (London)* **402**, 756 (1999).
- [2] For example, M. C. Facchini, M. Mircea, S. Fuzzi, and R. J. Charlson, *Nature (London)* **401**, 257 (1999).
- [3] For example, D. S. Jenkinson, K. Goulding, and D. S. Powlson, *Nature (London)* **400**, 629 (1999).
- [4] W. A. M. N. Smith, S. A. Thorpe, and A. Graham, *Nature (London)* **400**, 251 (1999).
- [5] P. L. Richardson, *Am. Sci.* **81**, 261 (1993).
- [6] P. R. ten Wolde and D. Frenkel, *Science* **277**, 1975 (1997).
- [7] L. da Vinci, *Codex on the flight of birds* (c. 1505), from anatomical manuscripts and drawings in the Royal Library, Windsor Castle, reproduced in C. Pedretti, *Leonardo, The Machines* (Giunti, Florence, Italy, 1999), p. 48.
- [8] D. Leighton and A. Acrivos, *J. Fluid Mech.* **177**, 109 (1987).
- [9] H. S. Husain, F. Hussain, and M. Goldshtik, *Phys. Rev. E* **52**, 4909 (1995).
- [10] M. R. Maxey, *Philos. Trans. R. Soc. London A* **333**, 289 (1990).
- [11] R. Gore and C. T. Crowe, *Int. J. Multiph. Flow* **15**, 279 (1989).
- [12] P. D. Swanson, F. J. Muzzio, A. Annapragada, and A. Adjei, *Int. J. Pharm.* **142**, 33 (1996); M. Liu, R. L. Peskin, and F. J. Muzzio, *Phys. Rev. E* **50**, 4245 (1994).
- [13] J. C. Sommerer and E. Ott, *Science* **259**, 335 (1993).
- [14] At low concentration, the red dye appears yellow in these photographs.
- [15] J. B. Weiss, *Phys. Fluids A* **3**, 1379 (1991).
- [16] Reduction in buoyancy is a well known result of stretching of a tracer solution; see, e.g., L. D. Landau and E. M. Lifshitz, *Fluid Mechanics* (Addison-Wesley, Reading, MA, 1959), p. 66.
- [17] For example, K. T. Alligood, T. D. Sauer, and J. A. Yorke, *Chaos: An Introduction to Dynamical Systems* (Springer, New York, 1997), p. 69.
- [18] Initial values used are  $C_0 = 0.64$ , and  $\Gamma = 0.99$ ; essentially similar results have been obtained for other parameter values.
- [19] Resonances [e.g., T. H. Solomon, E. R. Weeks, and H. L. Swinney, *Physica (Amsterdam)* **76D**, 70 (1994)] can carry tracers out of islands by the combined action of the map dynamics and buoyancy; however, typical trajectories farther than  $C_n/(1 - \Gamma)$  from a torus boundary remain trapped.
- [20]  $C_0 = 0.0064$ ,  $\Gamma = 0.99$ , and  $\tau = 400$  iterates. As before, 200 iterates of 500 initial points are plotted.
- [21] J. M. Zalc, M. M. Alvarez, B. E. Arik, and F. J. Muzzio, "Extensive Validation of Computed Laminar Flow Fields in a Stirred Tank Equipped with Three Rushton Turbines" (to be published).
- [22] Since we used  $5 \times 10^6$  tracers, calculating the full correlation function would in principle have required in excess of  $10^{11}$  calculations. We instead randomly selected  $5 \times 10^4$  tracers to compute the correlation functions shown [cf. R. C. Hilborne, *Chaos and Nonlinear Dynamics* (Oxford University Press, Oxford, U.K., 1994), p. 441].